Biochemical and Biophysical Research Communications 431 (2013) 232–238

Contents lists available at SciVerse ScienceDirect

Biochemical and Biophysical Research Communications

journal homepage: www.elsevier.com/locate/ybbrc

Insights into the mechanism of drug resistance: X-ray structure analysis of multi-drug resistant HIV-1 protease ritonavir complex

Zhigang Liu [a,b], Ravikiran S. Yedidi [a,c], Yong Wang [a], Tamaria G. Dewdney [a], Samuel J. Reiter [a], Joseph S. Brunzelle [d], Iulia A. Kovari [a], Ladislau C. Kovari [a,*]

[a] Department of Biochemistry and Molecular Biology, School of Medicine, Wayne State University, Detroit, MI 48201, USA
[b] Division of Internal Medicine, Harbor Hospital Baltimore, MD 21225, USA
[c] Experimental Retrovirology Section, HIV and AIDS Malignancy Branch, National Cancer Institute, National Institutes of Health Bethesda, MD 20892, USA
[d] Life Sciences Collaborative Access Team and Department of Molecular Pharmacology and Biological Chemistry, Northwestern University, Feinberg School of Medicine, Chicago, IL 60611, USA

ARTICLE INFO

Article history:
Received 27 December 2012
Available online 8 January 2013

Keywords:
HIV-1 protease
Multi-drug resistance
X-ray crystallography
IC50
Ritonavir

ABSTRACT

Ritonavir (RTV) is a first generation HIV-1 protease inhibitor with rapidly emerging drug resistance. Mutations at residues 46, 54, 82 and 84 render the HIV-1 protease drug resistant against RTV. We report the crystal structure of multi-drug resistant (MDR) 769 HIV-1 protease (carrying resistant mutations at residues 10, 36, 46, 54, 62, 63, 71, 82, 84 and 90) complexed with RTV and the *in vitro* enzymatic IC_{50} of RTV against MDR HIV-1 protease. The structural and functional studies demonstrate significant drug resistance of MDR HIV-1 protease against RTV, arising from reduced hydrogen bonds and Van der Waals interactions between RTV and MDR HIV-1 protease.

1. Introduction

Although neither a cure nor vaccine is available for HIV infection [1], the great success of highly active anti-retroviral therapy (HAART) has made it the treatment of choice against HIV viral replication since the mid 1990s [2]. Due to the absence of a proofreading function in reverse transcriptase [3], drug resistance mutations accumulate under the pressure of drug selection. Consequently, it is urgent to develop novel drugs to combat resistance [4].

An HIV-1 protease inhibitor is one of the components of HAART. Currently, there are ten FDA approved HIV-1 protease inhibitors in market. Most of these drugs contain a hydroxyethylene core and are peptidomimetic competitive inhibitors against the HIV-1 protease by mimicking the natural substrates [5–8]. Tipranavir, has a dihydropyrone ring as a central scaffold rather than a peptidomimetic hydroxyethylene core [9].

RTV is one of the first generation HIV-1 protease inhibitors approved by FDA in 1996. The 50% effective concentration (EC_{50}) of RTV to inhibit viral replication ranges between 3.8 and 153 nM depending on the viral isolate and culture cells. The recommended dosing schedule was twice a day due to a prolonged absorption and relatively long half-life [10]. The RTV monotherapy lead to a dramatic decrease of HIV-1 RNA plasma level and increase of CD4 cell count, although the anti-viral efficacy was shown to decline after 12–16 weeks of usage [11]. Further experiments showed signature mutations at positions 46, 54, 82 and 84 rendering HIV-1 protease drug resistant against RTV following long-term RTV monotherapy [12].

While crystal structures are available for RTV complexed with wild type and limited drug resistant HIV-1 protease [7,13,14], structural data is not available for RTV complexed with multi drug resistant HIV-1 protease. This structural information is essential to understand the drug resistance mechanism of the HIV-1 protease against RTV and could provide insights for resistance against other protease inhibitors.

To investigate the mechanism of RTV drug resistance, we have chosen a clinical isolate, MDR769 HIV-1 protease, as our study model. The high resolution crystal structure of MDR769 HIV-1 protease (PDB ID: 1TW7) with mutations at positions 10, 36, 46, 54, 62, 63, 71, 82, 84 and 90 [15,16] was solved previously by our group. 1TW7 exhibits an expanded active site cavity and wide-open flaps compared to wild type HIV-1 protease.

RTV was co-crystallized with MDR769 HIV-1 protease into space group $P4_1$, and the final structure was refined to 1.8 Å resolution.

Abbreviations: MDR, multi-drug resistance; HAART, highly active anti-retroviral therapy; RTV, ritonavir; IC_{50}, half maximal inhibitory concentration; RMSD, root mean square deviation.

* Corresponding author. Address: 540 E, Canfield Avenue, 4263 Scott Hall, Detroit, MI 48201, USA.
E-mail address: kovari@med.wayne.edu (L.C. Kovari).

0006-291X/$ - see front matter © 2013 Published by Elsevier Inc.
http://dx.doi.org/10.1016/j.bbrc.2012.12.127

This complex structure was then compared with WT HIV-1 protease ritonavir complex structure [7]. In addition, the *in vitro* IC_{50} of RTV against both WT and MDR769 HIV-1 protease was measured. These structural and functional studies show significant drug resistance of MDR HIV-1 protease against RTV, arising from the reduced interactions between RTV and MDR HIV-1 protease.

2. Materials and methods

2.1. Protein purification and co-crystallization

The inactive MDR769 HIV-1 A82T protease was over expressed by using a T7 promoter expression vector in conjunction with the *Escherichia coli* host, BL21 (DE3). Details of protein expression and purification were discussed in our previous research [17]. The active MDR769 HIV-1 protease was purified with the anion exchange resin chromatography pH at 7.8.

RTV was mixed with 2.5 mg/ml MDR769 HIV-1 A82T and diluted to 0.4 mM final concentration. The hanging drop vapor diffusion method was used to form the bi-pyramidal crystals of the MDR769 protease, with crystallization conditions published before [15].

2.2. Data collection and crystallographic refinement

The diffraction data were collected at 0.972 Å wavelength at the Advanced Photon Source (LS-CAT, beamline-21), Argonne National Laboratory. Data were reduced with CrystalClear. The X-ray diffraction data collection, processing parameters and structure refinement statistics are shown in Table 1. Molecular replacement was performed using Molrep-auto MR via CCP4 [18] with crystal structure previously solved in our lab [19] as a search model. Initial refinements were performed without RTV by Refmac5 [20]. The RTV molecule was built into the difference electron density maps as the refinement processed with program COOT [21]. Crystallographic waters were added with program ARP/wARP [22]. The structure was refined to resolution 1.8 Å with Refmac5. The final stereochemical parameters were checked using PROCHECK [23]. Images were generated using open source molecular graphics program, PyMol [24].

Table 1
Data collection and crystallographic refinement statistics.

Data collection	
Beam line	APS (LS-CAT 21)
Wavelength (Å)	0.972
Space group	$P4_1$
Cell dimension (Å) *a*, *b*, *c*	$a = b = 43.79$; $c = 99.45$
Resolution (Å)	26.43–1.65
R merge (%)[a]	9.0/38.7[b]
$I/\sigma(I)$	7.2/2.4
Redundancy	3.9/3.95
Completeness (%)	99.9/100.0
Unique reflections	22513
Refinement	
Resolution range (Å)	19.9–1.8
R_{work} (%)[c]	19.1
R_{free} (%)[d]	22.6
No. of protein atoms	1514
No. of water molecules	247
B factor	
Whole molecule	27.028
Side chain (includes water)	29.751
Main chain	23.524
Ligand	36.839
Solvent	39.51
RMSD	
Bond length	0.016
Bond angle	1.636
Ramachandran plot	
Favorable (%)	97.4
Additional (%)	2.6
Generous (%)	0
Forbidden (%)	0
PDB accession ID	4EYR

[a] $R_{merge} = \Sigma_{hkl}\Sigma_i|I_i(hkl) - \{I(hkl)\}|/\Sigma_{hkl}\Sigma_i I_i(hkl)$, where $I_i(hkl)$ is the intensity of an observation and I(hkl) is the mean value for its unique reflection. Summations cover all reflections.

[b] The values after the oblique indicate the highest resolution shell.

[c] $R_{work} = \Sigma_{hkl}||F_o| - |F_c||/\Sigma_{hkl}|F_o|$.

[d] R_{free} was calculated same way as *R* working, but with the reflections excluded from refinement. The *R* free set was chosen using default parameters in Refmac 5.

2.3. Analysis

PISA Server [25] was used to calculate the ligand binding energy in both MDR and WT HIV-1 protease RTV complexes. Hydrogen bonds that docked RTV were analyzed by PISA Server. The WT and MDR complexes were superposed using the Cα atoms of protease residues 1–99 and RMSD of Cα atoms was analyzed with the CCP4 program-Superpose Molecules. The solvent accessible area was calculated with the CCP4 program Accessible Surface Areas. The structural analyses were visualized using PyMol [24].

2.4. Enzyme assay

WT HIV-1 protease (NL4-3) was purchased from AnaSpec. Fluorescent substrate peptide, mimicking the natural substrate peptide MA/CA (matrix/capsid) with excitation/emission wavelength 340/490 nm, was dissolved in DMSO at concentration 500 μM. The composition of the fresh reaction buffer was 0.1 M sodium acetate, 1.0 M sodium chloride, 1.0 mM ethylenediaminetetraacetic acid (EDTA), 1.0 mM dithiothreitol (DTT), 10% dimethylsulfoxide (DMSO), and 1 mg/ml bovine serum albumin (BSA), with pH adjusted to 4.7. RTV was dissolved in DMSO at a stock concentration of 20 mM.

In each well of the 96 well flat bottom assay plate, 97 μl of reaction buffer was added first. 1 μl of HIV-1 protease was added to the buffer with the final concentration of 20 μM. 1 μl of RTV with different concentrations was added to the mixture. The whole reaction system was mixed gently and incubated at 37 °C for ten minutes. 1 μl of fluorescent substrate was added to reach the final concentration of 5 μM. The signal was recorded immediately by SpectraMax M5 from Molecular Devices at interval of one minute for twenty minutes at 37 °C. IC50 value was calculated with the program SoftMax Pro.

3. Results

3.1. Inhibition studies of RTV against WT and MDR HIV-1 protease

The IC_{50} of RTV was determined against both WT (NL4-3) and MDR HIV-1 protease for comparison. Fluorescent substrate peptide mimicking the natural substrate sequence MA/CA was added to monitor the enzyme activity.

IC_{50} values of RTV against WT and MDR769 HIV-1 protease were 0.34 ± 0.15 and 237 ± 5.6 nM, respectively. This result demonstrated a 697-fold resistance of MDR769 HIV-1 protease against RTV compared to WT HIV-1 protease. Supporting the drug resistance of MDR769 HIV-1 protease, the ΔG of the WT and MDR769 HIV-1 protease LPV complexes calculated by PISA server were −37.3 and −30.0 kcal/mol, respectively.

Compared to other HIV-1 protease mutant variants, MDR HIV-1 protease showed much higher degree of drug resistance to ritonavir. HIV-1 protease variants with mutations V82T/I84V, or M46I/

L63P/V82T/I84V were shown to be 158- and 150-fold resistance to RTV, respectively [26], while the MDR HIV-1 protease was 697-fold resistant to RTV.

3.2. Crystal structure of MDR769 HIV-1 protease RTV complex

RTV was co-crystallized with MDR769 HIV-1 protease into the space group $P4_1$ and the final structure was refined to resolution 1.8 Å with Refmac5. In each asymmetric unit, one protease dimer was observed. In addition, 247 crystallographic water molecules were observed in the complex. The electron density maps demonstrated two orientations of bound RTV to the MDR HIV-1 protease. The two RTV orientations were related by a pseudo-2-fold symmetry, and there was minimal asymmetry for the two orientations of RTV as was the case for the WT HIV-1 RTV complexes. To simplify the analysis, RTV was fit into the electron density map in one orientation with occupancy of 0.5. The data collection and refinement statistics are shown in Table 1.

3.3. Fewer hydrogen bonds in MDR HIV-1 protease RTV complex

Seven hydrogen bonds were noticed between RTV and MDR769 HIV-1 protease, while eight were observed in the WT HIV-1 protease RTV complex (Fig. 1 Panel A and B, Table 2). In addition, the hydrogen bond length in MD769 HIV-1 protease RTV complex was longer than those seen in WT HIV-1 protease RTV complex (pdb code 1HXW) [7]. Five out of the seven hydrogen bonds seen in MDR complex were also present in the WT HIV-1 protease RTV complex. Two new hydrogen bonds were observed in the MDR HIV-1 protease RTV complex: O61 to Asn 25 ND2 (monomer A, 3.81 Å) and O24 to Asn 25′ ND2 (monomer B, 3.58 Å). Moreover, in MDR HIV-1 protease RTV complex, the O41 formed hydrogen bonds only with Asn 25 OD1 (monomer A) and Asn 25′ OD1/ND2 (monomer B), while in the WT complex, the O41 formed four hydrogen bonds with Asp 25/25′ OD1/OD2, which more firmly secured the position of RTV.

Table 2
Hydrogen bonds mediating the RTV recognition in MDR and WT complexes.

Protein atom	MDR RTV complex		WT RTV complex	
	RTV atom	Length (Å)	RTV atom	Length (Å)
Asp 29 N	O76	2.82	O76	2.11
Asn 25OD1/Asp25OD1[a]	O41	3.04	O41	2.66
Gly 27 O	N58	3.34	N58	3.18
Asn 25 ND2	O61	3.81		
Gly 48 O			N20	3.12
Asn25′OD1/Asp25′OD1[b]	O41	2.83	O41	2.65
Asn25′ND2/Asp25′OD2	O41	2.88	O41	2.74
Asn25′ND2/Asp25′OD2	O24	3.58	N11	3.87
Gly 27′ O			N11	3.54

[a] In the MDR complex, the Asp 25/Asp 25′ was mutated to Asn 25/Asn 25′ to avoid auto-cleavage.
[b] The residues denoted by the symbol ′ indicate those from monomer B, while the residues without symbol ′ are those from monomer A.

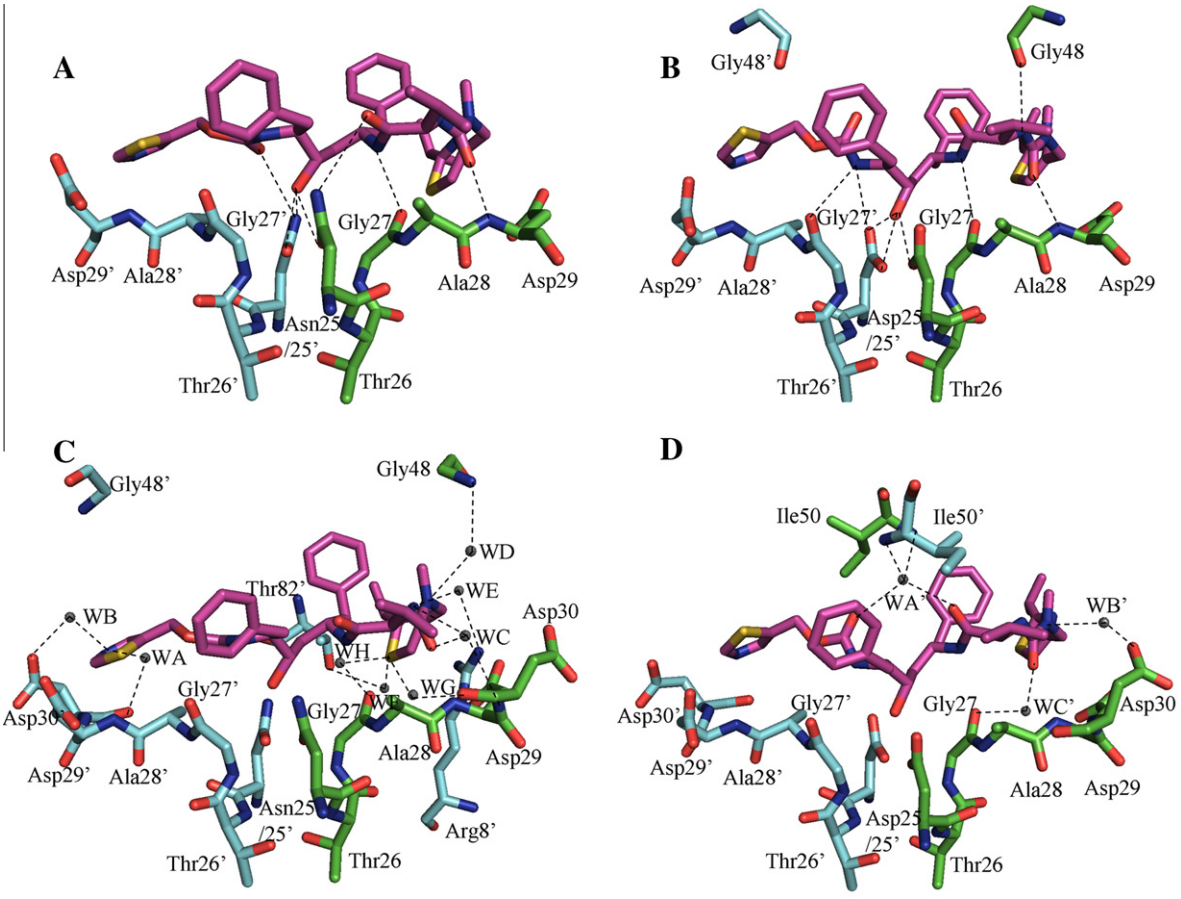

Fig. 1. Hydrogen bonds and crystallographic water molecules involved in RTV recognition and binding in both MDR (Panel A and C) and WT (Panel B and D) complexes (1HXW) [7]. RTV is shown in purple with stick model, and protease monomers are shown in green and cyan with stick model. The crystallographic water molecules are shown with gray sphere model. Hydrogen bonds between RTV and protease monomers are presented with dash line. (A) Hydrogen bonds mediating RTV recognition in MDR HIV-1 protease complex. (B) Hydrogen bonds mediating RTV recognition in WT HIV-1 protease complex. (C) Crystallographic water molecules and associated hydrogen bonds mediating RTV recognition in MDR HIV-1 protease complex. (D) Crystallographic water molecules and associated hydrogen bonds mediating RTV recognition in WT HIV-1 protease complex. (For interpretation of the references to color in this figure legend, the reader is referred to the web version of this article.)

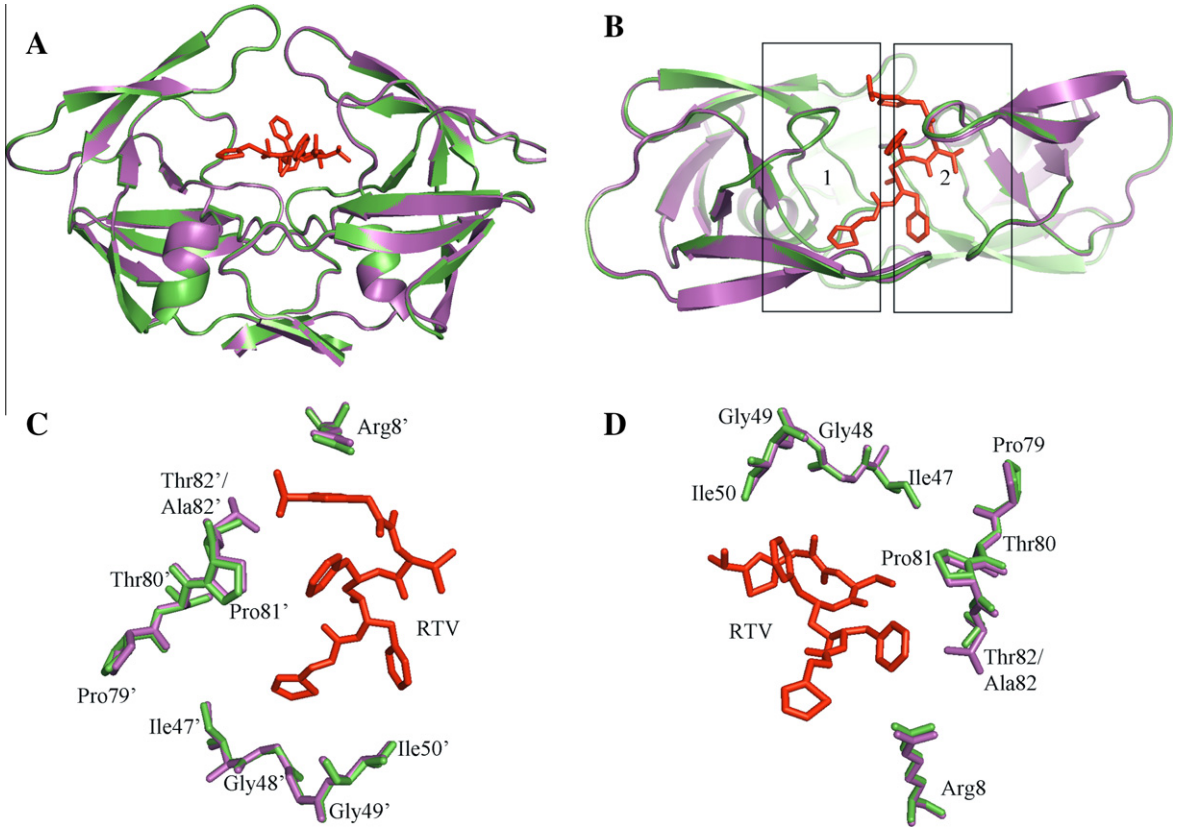

Fig. 2. Induced conformational changes of MDR HIV-1 protease upon the binding of RTV. RTV is represented with red stick model. Apo-MDR HIV-1 protease (1TW7) is shown in green color, while purple represents MDR HIV-1 protease complexed with RTV. (A) Front view of the superimposition of apo-MDR HIV-1 protease and MDR HIV-1 protease RTV complexes. (B) Top view of the superimposition of apo-MDR HIV-1 protease and MDR HIV-1 protease RTV complexes. (C) Conformational changes induced by RTV binding in the 80s loop, flap region and Arg 8′on monomer B, showing the details in box1. (D) Conformational changes induced by RTV binding in the 80s loop, flap region and Arg 8 on monomer A, showing the details in box 2. (For interpretation of the references to color in this figure legend, the reader is referred to the web version of this article.)

3.4. Fewer Van der Waals interactions in MDR HIV-1 protease RTV complex

Fewer Van der Waals interactions were found in MDR HIV-1 protease RTV complex compared to those in WT HIV-1 protease RTV complex. In MDR HIV-1 protease RTV complex, the ligand RTV formed 12 Van der Waals interactions with each of the protease monomers, A and B. In comparison, the number of Van der Waals interactions in the WT complex was 13 and 15, respectively [7]. In addition, in the MDR HIV-1 protease RTV complex, Gly 49 and Phe 53 from monomer A, Leu 10′, Gly 48′, Gly 49′ and Pro 81′ from monomer B were not involved in the Van der Waals interactions with RTV, while these residues were in direct contact with RTV in the WT complex via Van der Waals interactions.

3.5. Reduced surface area of RTV buried by MDR HIV-1 protease

In the MDR complex, 662.5 Å2 of RTV was inaccessible to solvent, which made up 69.03% of the total surface area. On the other hand, 811.5 Å2 surface area of RTV (84.8%) was buried by the protease in the WT complex [7]. The solvent accessible surface area of RTV when in complex with MDR 769 was increased by 15.8% compared to the WT due to the reduced hydrogen bonds and Van der Waals interactions. This finding supports our previous conclusion that MDR HIV-1 protease had an enlarged active site cavity.

3.6. Crystallographic water molecules involved in RTV recognition in MDR HIV-1 protease RTV complex

Crystallographic water molecules also participated in the ligand recognition in MDR HIV-1 protease RTV complex, as shown in Fig. 1 Panel C. In MDR HIV-1 protease complex, water A bridged RTV N5 and Asp 30′ O (monomer B). Water B bridged RTV N5 and Asp 30′ Oδ1 (monomer B). Water C bridged RTV N20 and Asp 30 N (monomer A), and also bridged RTV O76 and Asp 30 N (monomer A). Water D bridged RTV N74 and Gly 48 N (monomer A). Water E bridged RTV N83 and Arg 8′ NH2 (monomer B). Water F, G, H bridged RTV S81 and Thr 82′ Oγ1 (monomer B), Asp 29 Oδ2 (monomer A) and Gly 27 O (monomer A) respectively. Crystallographic water molecules with similar functions were also present in WT HIV-1 protease RTV complex. However, these crystallographic water molecules formed a less extensive network in the WT HIV-1 protease RTV complex than those did in the MDR HIV-1 protease RTV complex (Fig. 1 Panel C and D) [7].

The characteristic crystallographic water WA′, located between RTV and the two protease flaps [7], was not seen in MDR HIV-1 RTV complex. In the WT complex, this crystallographic water molecule bridged RTV atoms (O24 and O61) to Ile 50 N from either monomer. Absence of the flap-ligand bridging water molecule might explain partially the wide open nature of MDR HIV-1 protease flaps as well as the relatively weaker binding energy of RTV against MDR HIV-1 protease.

3.7. Induced conformational changes of MDR HIV-1 protease upon RTV binding

Superposition of MDR HIV-1 protease RTV complex and apo-MDR HIV-1 protease based on Cα revealed four high RMSD regions (Fig. 2 Panels A and B). Due to the binding of RTV, the 80s loop was attracted towards the active site cavity, making more contacts than otherwise as shown in Fig. 2 Panels C and D. The Cγ of Pro 81 moved 0.4 Å towards the active site cavity in the MDR complex. In addition, the shift of the 80s loop slightly closed the lateral opening of the active site cavity, formed by residues 81, 82 (monomer A), 8′, 47′, 48′, 49′, 50′ (monomer B), and made it less likely for RTV to slip out of the active site cavity from the lateral opening. However, the presence of RTV did not induce significant changes in the catalytic triad of residues 25, 26 and 27.

3.8. Wide open flaps of MDR HIV-1 protease despite RTV binding

The flaps were wide open in the MDR HIV-1 protease RTV complex. Contrary to the WT protease RTV complex, the binding of RTV did not close the flaps dramatically. The flap distance was measured from the Cα of Ile 50 in one monomer to the Cα of Ile 50 in the other monomer. The flap distance in the WT HIV-1 protease RTV complex was 5.9 Å [7]. In the apo-MDR HIV-1 protease, the flap distance was 12.2 Å, while the flap distance in the MDR HIV-1 protease RTV complex was 12.1 Å. The wide open flaps might contribute to the weaker binding of RTV to MDR HIV-1 protease, making it easier for RTV to be released from the active site cavity.

3.9. Increased dimerization area of MDR HIV-1 protease induced by RTV binding

The MDR HIV-1 protease dimer was further stabilized by the binding of RTV compared to apo-MDR HIV-1 protease. In the absence of RTV, the MDR HIV-1 protease dimerization area was 1330.9 Å^2. With RTV bound to MDR HIV-1 protease, the dimerization area increased by 12.5% to 1497.7 Å^2. In addition, the hydrogen bonds between the monomers increased from 23 in apo-MDR HIV-1 protease to 27 in the MDR HIV-1 protease RTV complex. Similarly, the salt bridges on the dimerization interface increased from 8 to 10 after the binding of RTV. However, compared to the WT HIV-1 protease RTV complex, the dimer was less stable in the MDR complex, considering the 1718.7 Å^2 of interface area in the WT complex [7]. Moreover, the dimer interface interaction composition was different between MDR and WT HIV-1 protease RTV complexes. In the MDR complex, there were 27 hydrogen bonds, 10 salt bridges and 19 Van der Waals interactions, while there were 19 hydrogen bonds, 8 salt bridges and 29 Van der Waals interactions in the WT complex. More detailed analysis of these interactions showed longer hydrogen bonds in MDR complex than those in WT complex.

4. Discussion

4.1. Semi-conserved Van der Waals interactions involving the 80s loop between WT and MDR HIV-1 protease RTV complexes

Although there is a significant conformational change of the 80s loop between MDR HIV-1 protease and WT HIV-1 protease RTV complexes, with Cα of Pro 81 in monomer A moving 1.6 Å, the Van der Waals interactions between RTV and the 80s loop in monomer chain A are conserved, due to the compensatory corresponding movement of RTV relative to the monomer A. In MDR HIV-1 protease RTV complex, C31, C32, C33, and C34 in RTV molecule form five Van der Waals interactions with Cγ2 and Cβ of Thr 82. Similarly, in WT HIV-1 protease RTV complex, C32, C33, C34 and C35 in RTV molecule form six Van der Waals interactions with Cγ1 of Val 82 and Cγ of Pro 81.

Table 3
Van der Waals interactions involving the 80s loop and Arg 8.

Protein atom	MDR RTV complex		WT RTV complex	
	RTV atom	Length (Å)	RTV atom	Length (Å)
Thr 82 Cγ2/Val 82 Cγ1[a]	C31	3.8	C32	4.2
	C32	3.0	C33	3.7
	C33	3.0	C34	3.6
	C34	3.8	C35	4.0
Thr 82 Cβ	C33	4.2		
Pro 81Cγ			C32	3.9
			C33	4.0
Thr 82′ Cγ2/Val 82′ Cγ2	S81	4.1	C45	3.8
	C82	4.2	C48	3.9
	C85	3.5	C49	4.0
	C90	3.8	C50	4.1
			C51	3.9
			C52	3.8
Thr 82′ Cβ/Val 82′ Cγ1	C85	3.7	S81	3.9
	C86	4.2		
	C90	4.1		
Pro 81′ Cγ	C50	4.2	C50	3.7
			C51	3.7
Pro 81′ Cδ			C51	4.0
Arg 8′ NH2	C75	3.7	C75	3.5
	C77	3.4	C77	3.5
	C80	3.5	C80	3.9
	S81	4.2	N83	3.9
	C82	4.1		
	N83	3.8		
Arg 8′ NH1	C80	4.2	C77	4.0
	S81	3.9	C80	3.9
	C82	4.0	S81	3.9
	C86	3.6	C82	4.0
			N83	4.0
Arg 8′ CZ	C77	3.9	C75	4.0
	C80	3.6	C77	3.6
	S81	3.8	C80	3.5
	C82	4.1	S81	4.1
	N83	4.1	N83	4.0
Arg 8′ NE	C80	3.8	C77	4.0
	S81	4.0	C80	3.5

[a] The residue 82/82′ in MDR HIV-1 protease is Thr, while it is Val in WT HIV-1 protease.

On the other hand, Van der Waals interactions vary between RTV and monomer B 80s loop between the WT [7] and MDR HIV-1 protease RTV complexes, as shown in Table 3. The Cα of Pro 81′ in monomer B moves 2.6 Å compared to the distance of 1.6 Å in monomer A. In MDR HIV-1 protease RTV complex, S81, C82, C85, and C90 in RTV molecule form 4 Van der Waals interactions with Thr 82′ Cγ2. C85, C86 and C90 form 3 Van der Waals interactions with Thr 82′ Cβ. In addition, C50 forms 1 Van der Waals interaction with Pro 81′ Cγ. On contrary, in WT HIV-1 protease RTV complex, C45, C48, C49, C50, C51, and C52 from RTV form 6 Van der Waals interactions with Val82′ Cγ2. S81 forms 1 Van der Waals interaction with Val 82′ Cγ1. C50 and C51 form 2 Van der Waals interactions with Pro 81′ Cγ. Furthermore, C51 forms 1Van der Waals interaction with Pro 81′ Cδ.

4.2. Conserved Van der Waals interactions involving Arg 8 between WT and MDR HIV-1 protease RTV complexes

The analysis of Arg 8/8′ in the RTV complex reveals highly conserved Van der Waals interactions between WT [7] and MDR HIV-1

protease RTV complexes, as shown in Table 3. No interaction is observed between RTV and Arg 8 from monomer A in either WT or MDR HIV-1 protease RTV complex. An extensive network of interaction between RTV and Arg8′ from monomer B is well established in both WT and MDR HIV-1 protease RTV complexes. C75, C77, C80, S81, C82 and N83 in RTV form 16 Van der Waals interactions with NH1, NH2, NE and CZ of Arg 8′ in both WT and MDR HIV-1 protease RTV complexes. C86 in RTV forms 1 Van der Waals interaction with Arg 8′ NH1 in MDR HIV-1 protease RTV complex only. Furthermore, the overall length of these Van der Waals interactions is slightly longer in MDR HIV-1 protease RTV complex compared to those in WT HIV-1 RTV complex. The length differences could be explained by the relative position of the RTV and Arg 8′ in both WT and MDR HIV-1 protease RTV complex. Compared to the WT protease, the CZ of Arg 8′ in monomer B moves about 1.6 Å towards the active site cavity, while the C82 atom of RTV moves 2.1 Å in the same direction in the MDR HIV-1 protease RTV complex. Consequently, the length of these Van der Waals is longer in MDR HIV-1 protease RTV complex, despite the conserved binding pattern.

4.3. Conformation changes of RTV between WT and MDR HIV-1 complexes

Major conformational changes are also found in the RTV molecule after the binding to WT [7] and MDR protease, despite the relative rigidity of RTV compared to the natural substrate peptides. These conformational changes in RTV modify the interactions between RTV and the protease. Although the conformation of RTV backbone is conserved between two complexes, the side chains, especially the ring structures, showed significant rotations to adjust the changes in protease (Fig. 3).

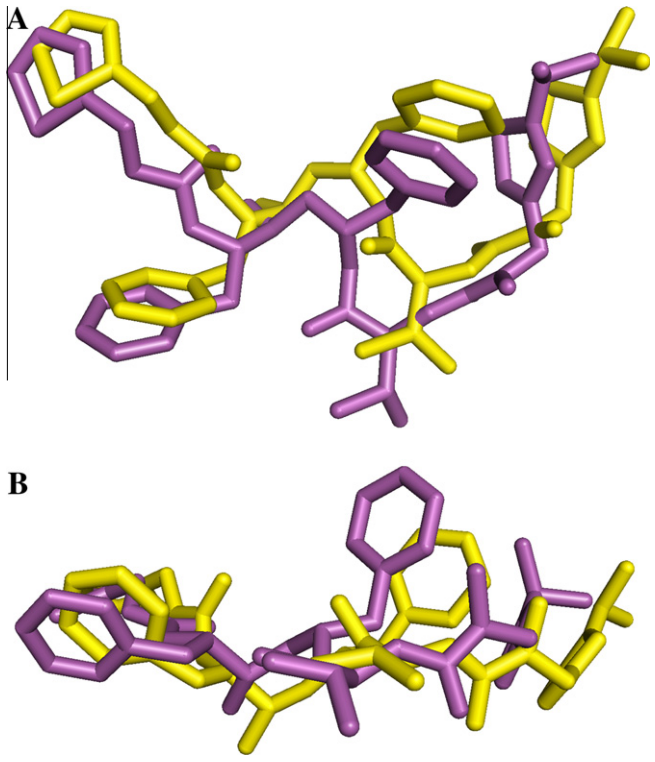

Fig. 3. Conformational changes (Panel A front view, Panel B top view) of RTV in MDR and WT HIV-1 protease RTV complexes [7]. RTV in MDR HIV-1 protease is shown in purple and RTV in WT HIV-1 protease is shown in yellow. (For interpretation of the references to color in this figure legend, the reader is referred to the web version of this article.)

4.4. Comparison between MDR HIV-1 protease RTV complex and HIV-1 protease V82A RTV complex

Crystallographic information is available for HIV-1 protease with limited drug resistant mutations, such as HIV-1 protease with mutation V82A complexed with RTV [13]. The comparison between our MDR and this V82A HIV-1 protease RTV complex reveals that: first, less interactions between RTV and HIV-1 protease V82A. But the reduction is not as significant as what we find in MDR HIV-1 protease RTV complexes. Second, RTV binding induces the closing of the flaps in the HIV-1protease V82A, while RTV binding does not affect the flap distance in MDR HIV-1 protease. Third, the characteristic crystallographic water WA′, locating between the two protease flaps and RTV is found in HIV-1 protease V82A RTV complex, but missing in MDR HIV-1 protease RTV complex.

Acknowledgments

This research was supported by the National Institutes of Health Grant AI65294 and a Grant from the American Foundation for AIDS Research (106457-34-RGGN).

References

[1] R.T. Schooley, J.W. Mellors, No cure yet for HIV-1, but therapeutic research presses on, J. Infect. Dis. 195 (2007) 770–772.
[2] G. Barbaro, A. Lucchini, G. Barbarini, Highly active antiretroviral therapy in HIV-associated pulmonary hypertension, Minerva Cardioangiol. 53 (2005) 153–154.
[3] Y. Takeuchi, T. Nagumo, H. Hoshino, Low fidelity of cell-free DNA synthesis by reverse transcriptase of human immunodeficiency virus, J. Virol. 62 (1988) 3900–3902.
[4] C. Sukasem, V. Churdboonchart, W. Sukeepaisarncharoen, W. Piroj, T. Inwisai, M. Tiensuwan, W. Chantratita, Genotypic resistance profiles in antiretroviral-naive HIV-1 infections before and after initiation of first-line HAART: impact of polymorphism on resistance to therapy, Int. J. Antimicrob. Agents 31 (2008) 277–281.
[5] J.A. Partaledis, K. Yamaguchi, M. Tisdale, E.E. Blair, C. Falcione, B. Maschera, R.E. Myers, S. Pazhanisamy, O. Futer, A.B. Cullinan, et al., In vitro selection and characterization of human immunodeficiency virus type 1 (HIV-1) isolates with reduced sensitivity to hydroxyethylamino sulfonamide inhibitors of HIV-1 aspartyl protease, J. Virol. 69 (1995) 5228–5235.
[6] J.C. Craig, I.B. Duncan, D. Hockley, C. Grief, N.A. Roberts, J.S. Mills, Antiviral properties of Ro 31-8959, an inhibitor of human immunodeficiency virus (HIV) proteinase, Antiviral Res. 16 (1991) 295–305.
[7] D.J. Kempf, K.C. Marsh, J.F. Denissen, E. McDonald, S. Vasavanonda, C.A. Flentge, B.E. Green, L. Fino, C.H. Park, X.P. Kong, et al., ABT-538 is a potent inhibitor of human immunodeficiency virus protease and has high oral bioavailability in humans, Proc. Natl. Acad. Sci. USA 92 (1995) 2484–2488.
[8] J.P. Vacca, B.D. Dorsey, W.A. Schleif, R.B. Levin, S.L. McDaniel, P.L. Darke, J. Zugay, J.C. Quintero, O.M. Blahy, E. Roth, et al., L-735,524: an orally bioavailable human immunodeficiency virus type 1 protease inhibitor, Proc. Natl. Acad. Sci. USA 91 (1994) 4096–4100.
[9] Y. Wang, Z. Liu, J.S. Brunzelle, I.A. Kovari, T.G. Dewdney, S.J. Reiter, L.C. Kovari, The higher barrier of darunavir and tipranavir resistance for HIV-1 protease, Biochem. Biophys. Res. Commun. 412 (2011) 737–742.
[10] S.A. Danner, A. Carr, J.M. Leonard, L.M. Lehman, F. Gudiol, J. Gonzales, A. Raventos, R. Rubio, E. Bouza, V. Pintado, et al., A short-term study of the safety, pharmacokinetics, and efficacy of ritonavir, an inhibitor of HIV-1 protease. European-Australian Collaborative Ritonavir Study Group, N. Engl. J. Med. 333 (1995) 1528–1533.
[11] M. Markowitz, M. Saag, W.G. Powderly, A.M. Hurley, A. Hsu, J.M. Valdes, D. Henry, F. Sattler, A. La Marca, J.M. Leonard, et al., A preliminary study of ritonavir, an inhibitor of HIV-1 protease, to treat HIV-1 infection, N. Engl. J. Med. 333 (1995) 1534–1539.
[12] J.C. Schmit, L. Ruiz, B. Clotet, A. Raventos, J. Tor, J. Leonard, J. Desmyter, E. De Clercq, A.M. Vandamme, Resistance-related mutations in the HIV-1 protease gene of patients treated for 1 year with the protease inhibitor ritonavir (ABT-538), AIDS 10 (1996) 995–999.
[13] M. Prabu-Jeyabalan, E.A. Nalivaika, N.M. King, C.A. Schiffer, Viability of a drug-resistant human immunodeficiency virus type 1 protease variant: structural insights for better antiviral therapy, J. Virol. 77 (2003) 1306–1315.
[14] J.C. Clemente, R.E. Moose, R. Hemrajani, L.R. Whitford, L. Govindasamy, R. Reutzel, R. McKenna, M. Agbandje-McKenna, M.M. Goodenow, B.M. Dunn, Comparing the accumulation of active- and nonactive-site mutations in the HIV-1 protease, Biochemistry 43 (2004) 12141–12151.
[15] Z. Liu, Y. Wang, J. Brunzelle, I.A. Kovari, L.C. Kovari, Nine crystal structures determine the substrate envelope of the MDR HIV-1 protease, Protein J. 30 (2011) 173–183.

[16] R.S. Yedidi, G. Proteasa, J.L. Martinez, J.F. Vickrey, P.D. Martin, Z. Wawrzak, Z. Liu, I.A. Kovari, L.C. Kovari, Contribution of the 80s loop of HIV-1 protease to the multidrug-resistance mechanism: crystallographic study of MDR769 HIV-1 protease variants, Acta Crystallogr. D: Biol. Crystallogr. 67 (2011) 524–532.
[17] J.F. Vickrey, B.C. Logsdon, G. Proteasa, S. Palmer, M.A. Winters, T.C. Merigan, L.C. Kovari, HIV-1 protease variants from 100-fold drug resistant clinical isolates: expression, purification, and crystallization, Protein Expr. Purif. 28 (2003) 165–172.
[18] The CCP4 suite: programs for protein crystallography, Acta Crystallogr. D: Biol. Crystallogr. 50 (1994) 760–763.
[19] B.C. Logsdon, J.F. Vickrey, P. Martin, G. Proteasa, J.I. Koepke, S.R. Terlecky, Z. Wawrzak, M.A. Winters, T.C. Merigan, L.C. Kovari, Crystal structures of a multidrug-resistant human immunodeficiency virus type 1 protease reveal an expanded active-site cavity, J. Virol. 78 (2004) 3123–3132.
[20] G.N. Murshudov, A.A. Vagin, E.J. Dodson, Refinement of macromolecular structures by the maximum-likelihood method, Acta Crystallogr. D: Biol. Crystallogr. 53 (1997) 240–255.
[21] P. Emsley, K. Cowtan, Coot: model-building tools for molecular graphics, Acta Crystallogr. D: Biol. Crystallogr. 60 (2004) 2126–2132.
[22] V.S. Lamzin, K.S. Wilson, Automated refinement of protein models, Acta Crystallogr. D: Biol. Crystallogr. 49 (1993) 129–147.
[23] A.A. Vaguine, J. Richelle, S.J. Wodak, SFCHECK: a unified set of procedures for evaluating the quality of macromolecular structure-factor data and their agreement with the atomic model, Acta Crystallogr. D: Biol. Crystallogr. 55 (1999) 191–205.
[24] W.L. DeLano, The PyMOL Molecular Graphics System (2002) DeLano Scientific, San Carlos, CA, USA. Available from: <http://www.pymol.org>
[25] E. Krissinel, K. Henrick, Inference of macromolecular assemblies from crystalline state, J. Mol. Biol. 372 (2007) 774–797.
[26] H.B. Schock, V.M. Garsky, L.C. Kuo, Mutational anatomy of an HIV-1 protease variant conferring cross-resistance to protease inhibitors in clinical trials. Compensatory modulations of binding and activity, J. Biol. Chem. 271 (1996) 31957–31963.